Dual Phase Separation for Synthesis of Bimodal Meso-/Macroporous Carbon Monoliths

Chengdu Liang and Sheng Dai*

Chemical Sciences Division and Center for Nanophase Materials Sciences, Oak Ridge National Laboratory, Oak Ridge, Tennessee 37831-2601

Received February 5, 2009. Revised Manuscript Received March 9, 2009

Polymerization-induced spinodal decomposition was conducted in glycolic solutions of phloroglucinol/formaldehyde copolymer and poly(ethylene oxide)−poly(propylene oxide)−poly(ethylene oxide) (PEO−PPO−PEO) to synthesize bicontinuous macroporous morphologies with microdomains from 0.5 to 6 μm. The polymeric materials were further carbonized at elevated temperature to yield bimodal meso-/macroporous carbon monoliths after the thermal decomposition of the PEO−PPO−PEO template. The bimodal porous nature of the resultant carbon monoliths was derived from the dual phase separation in which spinodal decomposition and microphase separation occurred simultaneously. We demonstrated the tunability of macropores without alteration of mesopore sizes.

Introduction

The immense scientific and commercial value of porous carbon materials is illustrated by their ubiquity as key materials in fuel cells, batteries, catalysts, and separation media.[1] The combination of meso- and macroporosities in bimodal porous carbons confers enhanced electronic,[2,3] mechanical,[3] and mass-transport[4] properties to sorbents due to the facilitated mass transport through the macropores while furnishing a high specific surface area through mesopores.[5] Mesoporous carbons are traditionally synthesized through various activation methods, which result in carbons of broad pore-size distributions (PSD) with complementary micro- and macropores. In recent years, the template-assisted synthesis opens an avenue for rational synthesis of mesoporous carbon with well-controlled pore sizes, morphologies, and symmetries.[1] According to the nature of templates, synthesis methods can be classified as hard-template[6] and soft-template synthesis.[1] The hard-template synthesis, also known as nanocasting, uses presynthesized mesoporous oxides and nanoparticles to shape the resultant carbon materials and the pores are formed after chemical etching of the hard templates. While the hard-template synthesis suffers from a tedious procedure during the preparation and removal of templates, soft-templates synthesis offers a handy synthesis approach through the self-assembly of carbon precursors with block copolymers and surfactants, which are sacrificed as porogens during carbonization. The underpinning physics of block copolymer self-assembly is the microphase separation,[7] which has been well-documented over the past few decades. A large variety of highly ordered mesoporous materials were synthesized by using the microphase separation phenomenon of block copolymers.

Spinodal decomposition is a well-established phase separation method for the synthesis of macroporous polymers with a macropore size in the low micrometer range.[8] To induce phase separation in a polymer system, two basic methods have developed. One is thermally induced phase separation and another is chemically induced phase separation.[8] Thermally induced phase separation is carried out in a polymer solution in which the phase diagram exhibits an upper critical solution temperature. The polymer forms a homogeneous solution when it has been heated to the upper critical solution temperature. The homogeneous solution can be induced to phase separation by thermal quenching to fall into the binodal or spinodal line, thus resulting in a two-phase morphology. Depending on the quench rate and the composition, phase separation occurs via either nucleation and growth or spinodal decomposition. Complete knowledge of kinetics and thermodynamics is required for control of the phase separation system. Because of the limit of heat-exchange rates, thermally induced phase separation is suitable only for the preparation of thin films, where a fast heat transfer from a heated solution to the environment can be achieved. Chemically induced phase separation is also called polymerization-induced phase separation.[9−13] To carry out the chemically induced phase separation, reactive precursors

* Corresponding author. E-mail: dais@ornl.gov.

(1) Liang, C.; Li, Z.; Dai, S. *Angew. Chem., Int. Ed.* **2008**, *47*, 3696–3717.
(2) Wang, D. W.; Li, F.; Liu, M.; Lu, G. Q.; Cheng, H. M. *Angew. Chem., Int. Ed.* **2008**, *47*, 373–376.
(3) Wang, Z. Y.; Li, F.; Ergang, N. S.; Stein, A. *Chem. Mater.* **2006**, *18*, 5543–5553.
(4) Liang, C. D.; Dai, S.; Guiochon, G. *Anal. Chem.* **2003**, *75*, 4904–4912.
(5) Nakanishi, K.; Tanaka, N. *Acc. Chem. Res.* **2007**, *40*, 863–873.
(6) Ryoo, R.; Joo, S. H.; Kruk, M.; Jaroniec, M. *Adv. Mater.* **2001**, *13*, 677–681.
(7) Bates, F. S.; Fredrickson, G. H. *Annu. Rev. Phys. Chem.* **1990**, *41*, 525–557.
(8) Kiefer, J.; Hedrick, J. L.; Hilborn, J. G. In *Macromolecular Architectures*; Springer-Verlag: Berlin, 1999; Vol. 147, pp 161−247.
(9) Fond, C.; Kiefer, J.; Mendels, D.; Ferrer, J. B.; Kausch, H. H.; Hilborn, J. G. *J. Mater. Sci.* **1998**, *33*, 3975–3984.
(10) Kiefer, J.; Kausch, H. H.; Hilborn, J. G. *Polym. Bull.* **1997**, *38*, 477–483.
(11) Kiefer, J.; Hilborn, J. G.; Hedrick, J. L. *Polymer* **1996**, *37*, 5715–5725.

10.1021/cm900344h CCC: $40.75
Published on Web 04/27/2009

are mixed with nonreactive low molecular weight or oligomeric solvents. The selection of a solvent or a mixture of solvents is very crucial, as a moderate solvent is required for the reactive precursors to give a homogeneous solution in the initial stage and becomes an immiscible solvent for the polymerized reactive precursors to obtain a phase-separated final morphology. Unlike the thermally induced phase separation that develops in a very rapid thermal quenching process, chemically induced phase separation is a relatively slow process in which the phase separation develops progressively during the polymerization of the precursor. The growth or cross-linking of the polymer chains results in the immiscibility of the cured polymer and the nonreactive solvents. Consequently, the initial solvent becomes a nonsolvent in liquid droplets to form a secondary phase, which eventually forms voids for the cured porous polymer. The chemically induced phase separation is less understood than thermally induced phase separation due to the theoretical complexity of this method.[8] Nonetheless, chemically induced phase separation has been widely utilized in the preparation of porous polymers in forms from thin films to large monoliths. When poly(furfuryl alcohol), a polymeric carbon precursor, was employed, uniform macropores that developed in the spinodal decomposition process were retained after pyrolysis at a temperature higher than 800 °C. Uniform macroporous carbons were successfully prepared with controlled pore sizes from 0.5 to 5 μm.[14]

A dual phase separation process,[5] which combines the microphase separation and spinodal decomposition, was first reported as a versatile method for the synthesis of bimodal porous silicate and hybrid silicate materials that have a hierarchical porosity of two discrete length scales in nanometers and micrometers. The hierarchically meso-/macroporosity of these silicate materials results from the concurrent presence of microphase separation and spinodal decomposition. Later on, we patented the dual phase separation method for the synthesis of carbon monolith with an application for monolithic liquid chromatography columns.[15] Although bimodal porous carbon can be synthesized through replication of bimodal porous silica monolith[16,17] and combined hard−soft templating synthesis,[18] a one-step synthesis could simplify the synthesis procedure as reported by Zhao and co-workers with a hydrothermal synthesis process.[19] In spite of the simplicity of the synthesis procedure, the dual phase separation synthesis has its complex physiochemical changes resulting from the coupled phase separations. Due to the limited publications about this emerging method, the physics of the dual phase separation is largely unknown. How do the two phase separations interplay with each other? How can this dual phase separation phenomenon be harnessed for controlled synthesis of materials by design? We report herein a facile synthesis approach for bimodal porous carbon through a dual phase separation process by which the tunability of the macropores was demonstrated while the size of the mesopores remained unchanged.

Table 1. Synthesis Conditions Investigated[a]

sample ID	ratio	solvent	T1	T2	T3	temp (°C)
MC1	0.5:1	TEG	70 min	12 h		96
MC2	1:1	TEG	70 min	12 h		96
MC3	2:1	TEG	70 min	12 h		96
MC4	3:1	TEG	70 min	12 h		96
MC5	4:1	TEG	70 min	12 h		96
MC6	3:1	TEG	30 min	12 h		96
MC7	3:1	TEG	40 min	12 h		96
MC8	3:1	TEG	60 min	12 h		96
MC9	3:1	TEG	80 min	12 h		96
MC10	3:1	TEG	90 min	12 h		96
MC11	3:1	EG	70 min	12 h		96
MC12	3:1	DG	70 min	12 h		96
MC13	3:1	DG/TEG 1:1	70 min	12 h		96
MC14	3:1	TetraEG	70 min	12 h		96
MC15	3:1	TEG	70 min	12 h		80
MC16	3:1	TEG	70 min	12 h		100
MC17	3:1	TEG	70 min	12 h		110
MC18	3:1	TEG	70 min	8 h	12 h	96

[a] Ratio: ratio of polymer to solvent. Solvent: pure and mixtures of solvents; EG, ethylene glycol; DEG, diethylene glycol; TEG, triethylene glycol; TetraEG, tetraethelyene glycol; T1, prepolymerization time (min); T2, time in air bath (h); T3, aging time (h); temp, air-bath temperature (°C).

Experimental Section

Chemicals. Triblock poly(ethylene oxide)-*b*-poly(propylene oxide)-*b*-poly(ethylene oxide) copolymer Pluronic F127 ($EO_{106}PO_{70}EO_{106}$, M_v = 12600), ethylene glycol (EG), diethylene glycol (DEG), triethylene glycol (TEG), and tetraethylene glycol (TetraEG), hydrochloride acid (37 wt % aqueous solution), phloroglucinol (HPLC grade), and formaldehyde (37 wt % aqueous solution) were purchased from Aldrich. Ethanol (200 proof) was a product of Pharmco Aaper Inc. distributed by ORNL local store. Deionized (DI) water was generated by a Millipore water purification system. All chemicals were used as received.

Synthesis of Polymeric Materials. A prepolymerization step was conducted for the synthesis of a polymeric mixture of phloroglucinol/formaldehyde copolymer and triblock copolymer F127 according to a previous publication.[20] Briefly, 1.26 g of phloroglucinol, 1.26 g of F127, 0.1 g of 37 wt % hydrochloride acid solution, 5 g of ethanol, and 4 g of water were mixed and stirred until they became a homogeneous solution with a water bath at 30 °C. Subsequently, 1.3 g of formaldehyde (37 wt % aqueous solution) was added to the mixture under stirring. The prepolymerization was conducted for 30−90 min. The duration of prepolymerization was recorded as T1. The polymer phase was separated from the solvents after the polymerization by centrifugation at 9500 rpm for 5 min. A portion of prepolymerized mixture was then dissolved in glycolic solvents and immediately transferred into a glass tube (7 mm inner diameter, 30 cm long). The glass tube was sealed and placed in an air bath heated at temperatures specified in Table 1. All samples were heated in the air bath for 12 h with exception of sample MC18, which was washed with

(12) Kiefer, J.; Hilborn, J. G.; Manson, J. A. E.; Leterrier, Y.; Hedrick, J. L. *Macromolecules* **1996**, *29*, 4158–4160.
(13) Pascault, J. P. *Macromol. Symp.* **1995**, *93*, 43–51.
(14) Constant, K. P.; Lee, J. R.; Chiang, Y. M. *J. Mater. Res.* **1996**, *11*, 2338–2345.
(15) Dai, S.; Guiochon, G. A.; Liang, C. Robust carbon monolith having hierarchical porosity. U.S. Patent 7449165, Nov 11, 2008; 2005169829.
(16) Taguchi, A.; Smatt, J. H.; Linden, M. *Adv. Mater.* **2003**, *15*, 1209–1211.
(17) Shi, Z. G.; Feng, Y. Q.; Xu, L.; Da, S. L.; Zhang, M. *Carbon* **2003**, *41*, 2677–2679.
(18) Alvarez, S.; Fuertes, A. B. *Mater. Lett.* **2007**, *61*, 2378–2381.
(19) Huang, Y.; Cai, H. Q.; Feng, D.; Gu, D.; Deng, Y. H.; Tu, B.; Wang, H. T.; Webley, P. A.; Zhao, D. Y. *Chem. Commun.* **2008**, 2641–2643.
(20) (a) Liang, C. D.; Dai, S. *J. Am. Chem. Soc.* **2006**, *128*, 5316–5317. (b) Wang, X. Q.; Liang, C. D.; Dai, S. *Langmuir* **2008**, *24*, 7500–7505.

copious TEG after being heated for 8 h and then aged in TEG at 100 °C for 12 h. After the polymer rods were released from the glass tubes, the fluffy precipitates on the rod surfaces were wiped off. The glycolic solvents were washed off by soaking the samples in ethanol for 4 h and then exchanged with DI water. All rods were dried in air for 4 h and then held inside a glass tube dried at 100 °C overnight. The detailed synthesis conditions were tabulated in Table 1.

Carbonization. Each polymer rod was held inside a fused silica tube with an inner diameter slightly larger than the outer diameter of the polymer rod. The polymer rods along with the silica tubes were then loaded into a tube furnace (Thermolyne, Model 79300). A stream of house nitrogen was fed through one end of the tube furnace at 50 sccm during the entire course of carbonization. The samples were heated to 850 at 2 °C/min and held at 850 °C for 2 h. All samples were unloaded after the furnace cooled down to room temperature.

High-Temperature Treatment. The high-temperature treatment was conduced on a graphite furnace (Thermal Technology Inc., Model 1000-2560-P20). All samples were degassed through three cycles of evacuation and refilling of helium gas after they had been loaded into the furnace. The heating treatment was carried out at a slightly positive pressure of 5 mmHg under the protection of a helium stream at 5 sccm. The furnace was ramped to 2600 at 40 °C/min and held for 1 h. Samples were discharged after the heating chamber cooled to room temperature.

Characterization. The low-magnification images were taken in a scanning electron microscope (SEM, Model JEOL 6060) system that operated at 15 kV. The high-magnification images were imaged by a scanning transmission electron microscope (STEM HD-2000). Small pieces of sample were sandwiched between two transmission electron microscopic (TEM) grids and loaded into the column through a standard TEM sample holder. The STEM unit was operated at an electron accelerating voltage of 200 kV and an emission current of 30 μA. Nitrogen sorption isotherms of the porous carbons were measured at 77 K using a Micromeritic Gemini 275 system. The specific surface areas and pore size distributions were calculated by using the Brunauer−Emmett−Teller (BET) theory and the Barrett−Joyner−Halenda (BJH) method based on the adsorption branches of the isotherms. The specific pore volumes were measured at relative pressure 0.95. The thermogravimetric analysis (TGA) was conducted on a TA Q-500 TGA system (TA Instruments). Platinum pans were preheated to 1000 °C in air for 2 h and cooled to room temperature prior to loading of the samples. All TGA measurements were run under nitrogen from room temperature to 850 °C through a ramp of 2 °C/min. Powder X-ray diffraction (PXRD) patterns were recorded on a PANalytical X'pert PRO 2-circle X-ray diffractometer. The samples were ground by a mortar and pestle and loaded onto a silicon zero-background sample holder.

Results

General Description of Bimodal Porous Carbon Monolith. The representative microstructure of a typical bimodal porous carbon is shown in Figure 1 B,C, which reveal a bicontinuous network of carbon with a macropore size of ~3 μm, skeletal size of 1 μm, and mesopores of 8 nm. The network fully developed after the polymerization as shown in the comparison between parts (A) and (B) of Figure 1, which were taken from the polymeric material before carbonization and the carbon material resulting from carbonization of the polymeric material, respectively. The microstructural patterns in Figure 1A,B are similar but the

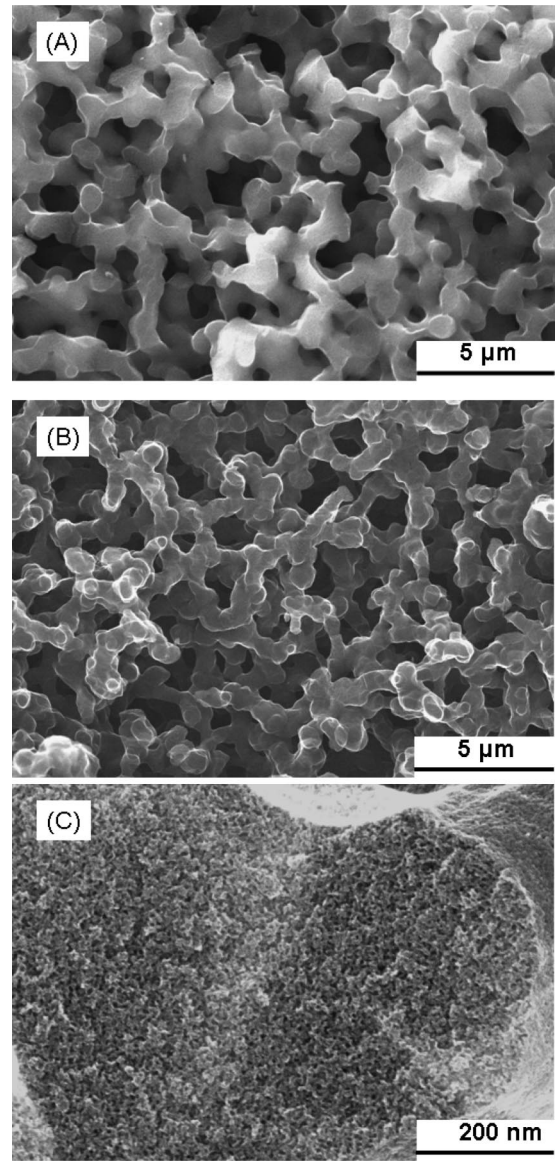

Figure 1. Microstructure of sample MC4: (A) bicontinuous network of the polymeric material before carbonization; the image was taken after physical vapor deposition of gold for the elimination of charging. (B) Bicontinuous network of carbon. (C) Mesopores on the skeleton of the carbonized sample. Scale bars are specified in images.

size of the domains in Figure 1 B is smaller than that in Figure 1A because of the dimensional shrinkage upon carbonization. The mesopores in the skeleton of the carbon was visualized by a high-resolution SEM image in Figure 1C. Because a directly micrographic comparison of the polymer skeleton and carbon skeleton was difficult to make due to the severe charging of the polymeric materials under high-resolution SEM, the mesopores were measured and compared by BET measurements of N_2 uptake at 77 K. The isotherms were plotted in Figure 2. The polymer rods (dotted blue line) adsorbed a negligible amount of N_2, while the carbonized sample (heated to 850 °C, solid black line) and graphitized sample (heated to 2600 °C, dashed red line) showed sharp steps of N_2 uptake at relative pressure between 0.6 and 0.8. Evidently, the mesopores developed after carbonization.

The sizes and morphologies of the macropores and skeletons of the resulting carbons depend on the synthesis

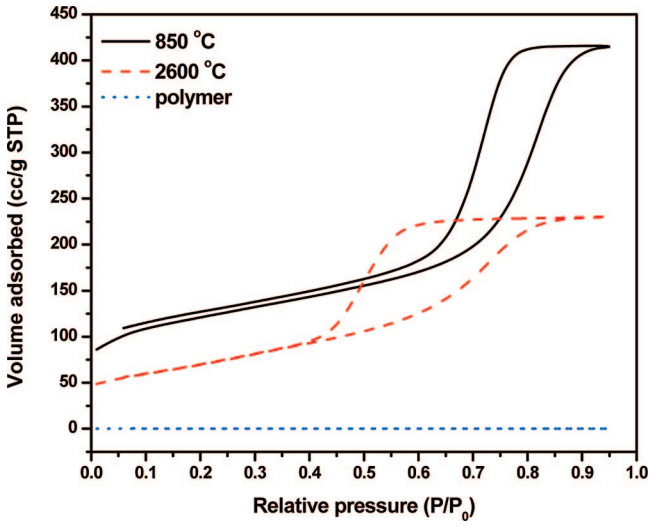

Figure 2. BET isotherms of sample MC4 at different stages: (1) the polymer rod (dotted blue line); (2) the carbon rod carbonized at 850 °C (solid black line); (3) the carbon rod heated to 2600 °C (dashed red line).

conditions. We set sample MC4 as a reference recipe for the synthesis condition. Based on the reference, we systematically investigated the major factors that significantly affected the phase separation, including the duration of prepolymerization, solvent, ratio of solvent to polymer, and temperature. Wall effect was observed and eliminated by an optimized synthesis condition. A complete description of the resulting carbon was summarized in Table 2 including characteristics of the microstructures and the time when the clouding point appeared after being heated in the air bath. The morphologies of macropores were described in detail according to the factors under investigation.

Morphologies of Macropores and Skeletons. *Effect of Prepolymerization.* F127 is sparely soluble in the glycolic solvents under investigation at room temperature. The solubility of F127 in the glycolic solvents at elevated temperatures was not measured, but we observed two immiscible layers of liquids when the mixture of 1:4 (weight ratio) of F127 and glycolic solvents was heated to the temperature between 60 and 140 °C. After F127 and phloroglucinol were premixed and prepolymerized with formaldehyde in an ethanolic solution as we reported elsewhere,[20] The polymer mixture that separated from the ethanolic solution contained F127, oligomers of phloroglucinol/formaldehyde, and a small amount of ethanol and water. The resulting polymer mixture was miscible with glycolic solvents when the duration of prepolymerization was shorter than 120 min. The viscosity of the polymer mixture was a function of prepolymerization time. The long prepolymerization time resulted in viscous polymer mixtures due to the increase of average molecular weight of the phloroglucinol−formaldehyde oligomers. Apparently, small-size oligomers of phloroglucinol−formaldehyde promoted the miscibility of F127 and glycolic solvents. The duration of the prepolymerization affected the morphologies of the resulting polymer rods and the carbon monoliths. Samples MC6, MC7, MC8, MC4, MC9, and MC10 were synthesized with the same composition but with different durations of prepolymerization from 30 to 90 min. Figure 3 shows the morphologies of carbons resulting for MC6, MC7, MC8, MC4, MC9, and MC10. MC6 was prepolymerized for 30 min. This sample has the morphology of loose spherical particles with a broad size distribution from 1 to 20 μm (Figure 3A). When the duration of prepolymerization increased to above 40 min, the resulting materials shown from Figure 3B to Figure 4F have bicontinuous morphologies. The skeletal size of the carbon domains decreased while the prepolymerization time increased. Secondary phase separations were observed in samples MC7 and MC8, which were prepolymerized for 40 and 60 min, respectively. Spherical pores of about 1 μm presented in the skeleton of MC7. The spherical pores were voids left by the solvents that separated out in the polymer-rich domain as a result of the secondary phase separation. Carbon spheres were seen on the surface of the skeleton. Most likely, these carbon spheres were resulting from the secondary phase separation of polymers in the solvent-rich domain. These spherical particles landed on the surface of the skeleton after the removal of the glycolic solvents. The texture of MC8 is much finer than that of MC7. Although no macropore was observed on the skeleton, a few spherical particles that landed on the surface of the skeleton indicated the secondary phase separation in the solvent-rich phase. No secondary phase separation occurred in samples MC4, MC9, and MC10.

Influence of Solvent. Inspired by the work of Chiang and co-workers, who successfully synthesized macroporous carbon monoliths via a macrophase separation of poly(furfuryl alcohol) in triethylene glycol, we also utilized triethylene glycol and its derivatives as solvents for inducing macrophase separation in our phenolic polymer system. The similarity in the hydrophilicity of the furfuryl alcohol polymer system to that of our phenolic polymer system forms the key rationale for us to choose triethylene glycol and related solvents. Four glycolic solvents, ethylene glycol (EG), diethylene glycol (DEG), triethylene glycol (TEG), and tetraethylene glycol (TetraEG), were invested in the synthesis. Phase separation was observed when the polymerization was conduced in EG, DEG, TEG, and the mixture of DEG and TEG. The polymerization in TetraEG failed to produce any solid material. Shown in Figure 4 are SEM images taken from the carbon materials synthesized by using different solvents. These samples were denoted as MC11, MC12, and MC13, which were synthesized in EG, DEG, and TEG/DEG (1:1 ratio), respectively. For the purpose of comparison, an image of MC4 was also included in Figure 4. The material resulting from EG (Figure 4A) displayed a loose structure of spherical particles in the size region between 1 and 5 μm. Small particles agglomerated into large ones. Polymer and carbon rods were able to form but the materials were fragile. Figure 4B showed the microstructure of the carbon synthesized in DEG. A grainy skeleton was obtained with uniform grain size of about 1−2 μm. The grains were close to spheres and interconnected to form the network. Sample MC12 was stiffer than sample MC11 but less stiff than sample MC13 that was synthesized from the mixture of DEG and TEG. The morphology of MC13 was akin to that of MC12.

Table 2. Characteristics of the Microstructures and Clouding Points[a]

sample ID	T4	pore size (μm)	skeletal size (μm)	description of the structure evolved from spinodal decomposition
MC1	45 min	~1		isolated pore, <2 μm
MC2	1.4 h	~2		isolated pore, ~2 μm
MC3	2 h	<2	3−5	bicontinuous structure, coarse skeleton, pores are partially open
MC4	3.5 h	3	1	bicontinuous structure, completely open pores, fine skeleton
MC5	4.5 h			structure collapsed
MC6	30 min			spherical particles, 1−20 μm
MC7	2 h	>10	>10	bicontinuous structure, completely open pores, coarse skeleton with secondary phase separation in both polymer phase and solvent phase; the secondary phase separation resulted in pores in the skeleton and spherical particles in the primary pores
MC8	3.5 h	3	1	bicontinuous structure, completely open pores, fine skeleton; similar to sample MC4
MC9	5 h	2	<1	bicontinuous structure, partially open pores, fine skeleton
MC10	6 h	2	~0.5	bicontinuous structure, partially open pores, very fine skeleton
MC11	1 h			spherical particles, 1−5 μm
MC12	2 h			spherical particles, 1−2 μm
MC13	2.5 h			spherical particles, fused particles
MC14				failed to gel
MC15	2.5 h			spherical particles
MC16	5 h	~1	~0.5	bicontinuous structure, completely open pores, very fine skeleton
MC17				failed to gel
MC18	3.5 h	3	1	completely open pores, no wall effect observed

[a] T4, time when clouding point occurred after heating in the air bath.

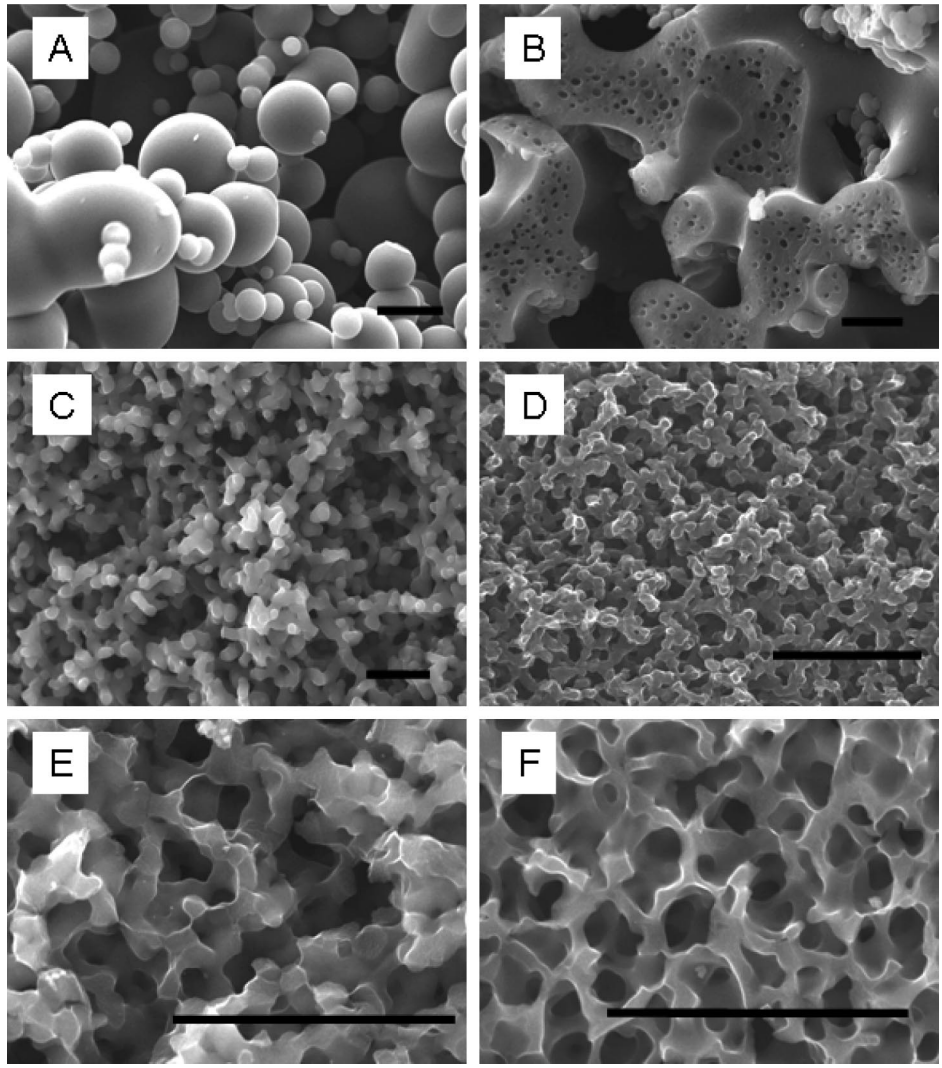

Figure 3. Morphologies of carbon samples as a function of the prepolymerization time: (A) 30 min, sample MC6; (B) 40 min, sample MC7; (C) 60 min, sample MC8; (D) 70 min, sample MC4; (E) 80 min, sample MC9; and (F) 90 min, sample MC10. Scale bars represent 10 μm.

Spherical particles of 1.5 μm were observed in MC13. These particles were fused into a continuous network with voids from 1 to 5 μm. Figure 4D is the microstructure of a reference sample (MC4) that was synthesized in TEG. MC4 had a highly ramified skeleton with smooth transitions. The sizes of the skeleton and macropores were about 1 and 3 μm, respectively. Differing from the morphologies of MC12 and MC13, the skeleton of MC4 did not have any feature

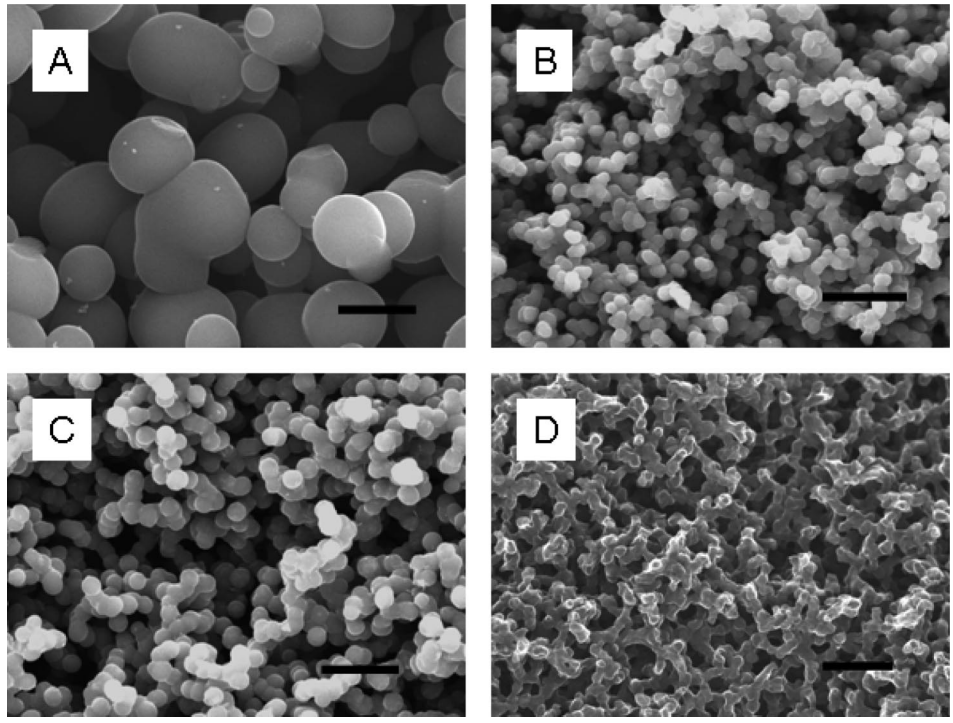

Figure 4. Morphologies of carbon monoliths synthesized by using different solvents: (A) ethylene glycol, sample MC11; (B) diethylene glycol, sample MC12; (C) diethylene glycol/triethylene glycol (1:1 weight ratio), sample MC13; and (D) triethylene glycol, sample MC4 (this is the sample set as the reference recipe). Scale bars represent 5 μm.

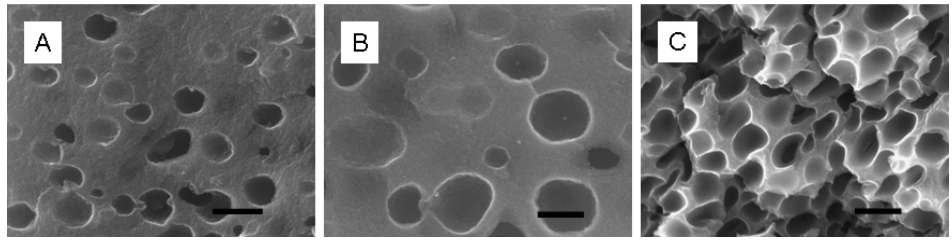

Figure 5. Microstructures of the carbon monolith synthesized with different ratios of solvent to polymer. The samples were synthesized with the weight ratios of TEG-to-polymer mixture: (A) 0.5:1, sample MC1; (B) 1:1, sample MC2; (C) 2:1, sample MC3. Scale bars represent 2 μm.

showing the spherical morphologies. Rigid polymer and carbon rods were obtained by using TEG as the solvent.

Solvent-to-Polymer Ratio. The solvent-to-polymer ratio affected the macropores and skeletons in three aspects: (1) the morphology of macropores, (2) the size of skeletons and macropores, and (3) the interconnectivity of the macropores. Spherical macropores developed when samples MC1 and MC2 were synthesized with a small ratio of solvent to polymer (Figure 5A,B). The macropores in these two samples scattered in the matrix of carbon without interconnectivity. The size of macropores in MC1 was about 1 μm and the macropores in MC2 doubled in size as the ratio of solvent to polymer doubled. When the ratio of solvent to polymer increased to 2:1, partially interconnected macropores developed (Figure 5C) in MC3. Cracks developed in the materials with isolated or partially interconnected macropores. Highly interconnected macropores can be synthesized when the solvent-to-polymer ratio was 3:1. Samples in Figures 3 and 4 were synthesized by using a solvent-to-polymer ratio of 3:1. No cracking was found in carbon samples with bicontinuous macropores. Further increasing of the solvent-to-polymer ratio of 4:1 gave rise to sample MC5 which failed to form a monolithic material.

Effect of Temperature. Both prepolymerization and cross-linking of phloroglucinol and formaldehyde were significantly affected by temperature. To simplify the synthesis process, we used a fixed temperature of 30 °C for the prepolymerization. The influence of temperature during the cross-linking of phloroglucinol/formaldehyde in TEG solvent was investigated at 80, 96, 100, and 110 °C. Spherical morphologies with skeleton sizes of about 10 μm developed when the air-bath temperature was 80 °C (sample MC15 in Figure 6A). When the bath temperature was increased to above 96 °C, a bicontinuous structure of nonspherical morphologies gradually developed. Finer structures were evolved at elevated temperatures. A macropore size of 3 μm and a skeleton size of 1 μm were synthesized at 96 °C (sample MC4), and a macropore size of 1 μm and a skeleton size of 0.5 μm were synthesized at 100 °C (sample MC16). With further increasing of the temperature to 110 °C, the solution failed to gel into a solid material. Fluffy polymeric materials were found on the surface of the polymer rods when the rods were removed out of the air bath. These fluffy polymeric materials can be scratched off the rod surface.

Wall Effect. The spinodal decomposition was found to be greatly influenced by the wall of the container. A so-called

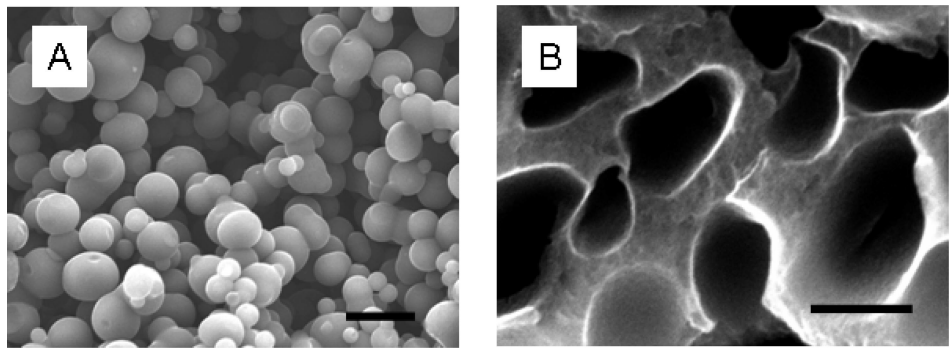

Figure 6. Microstructures of carbon monoliths synthesized at different temperatures. (A) 80 °C, sample MC15, scale bar represents 10 μm; and (B) 100 °C, sample MC16, scale bar represents 1 μm.

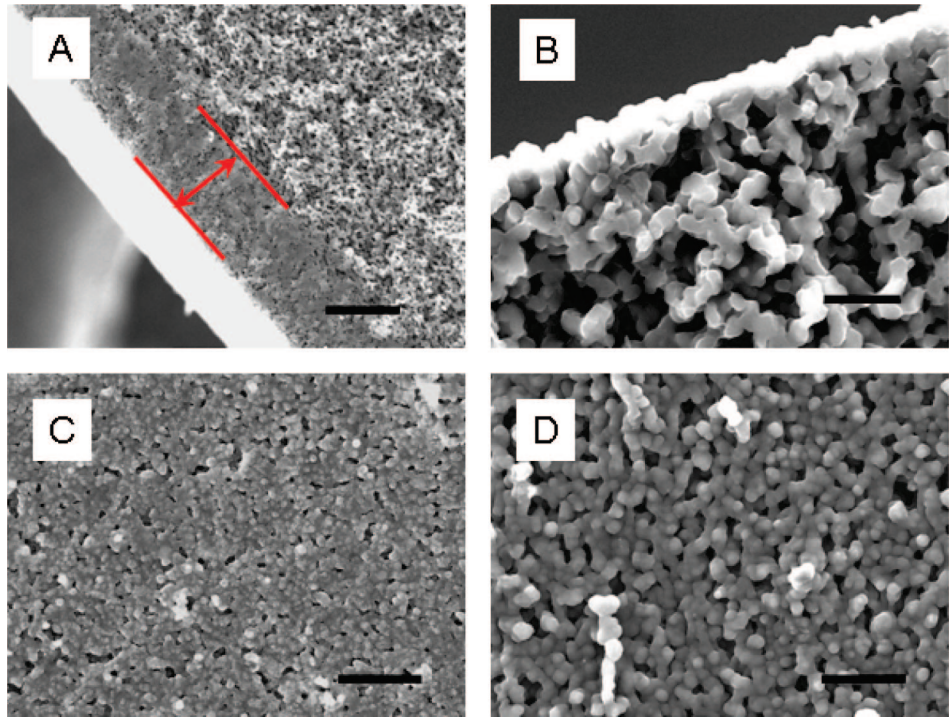

Figure 7. Heterogeneity induced by the wall effect: (A) Cross section of carbon monolith rod prepared according to the reference recipe, MC4. Red lines and arrows indicate the heterogeneity domain at the edge of the carbon rod. The thickness of the heterogeneity domain is about 20 μm. Scale bar represents 20 μm. (B) Cross section of carbon monolith rod without wall effect, sample MC18. Scale bar represents 5 μm. (C) Surface texture of sample MC4 with wall effect. (D) Surface texture of sample MC18 without wall effect. Scale bars in (C) and (D) represent 10 μm.

"wall effect" has been studied both theoretically and experimentally.[21] As a result of the wall effect, the sizes of domains near the wall differ from those away from the wall.[21−23] Heterogeneity in the skeletal structures was observed at the cross section of the carbon rods. In a typical preparation as described in the reference recipe for MC4, a layer of an ca. 20 μm thick heterogeneous region formed as the outmost shell of the carbon rods. This heterogeneous shell was visualized in Figure 7A that was indicated by red lines and an arrow. The texture of the shell was finer than the rest of the rods. The wall effect can be eliminated by aging the polymer rods in a pure solvent without contact of the glass tube. Sample MC18 was prepared according to the MC4 reference recipe except for the aging stage, which was conducted in TEG after the polymer rod was formed. No heterogeneous shell was found in the carbon rods prepared from sample MC18 as shown in Figure 7B. The surface texture of carbon rods from samples MC4 and MC18 were imaged at the same magnification and compared in parts (C) and (D), respectively, in Figure 7. Evidently; the wall effect resulted in a finer superficial grain size of MC4 than that of MC18.

Clouding Point. The commencement of the phase separation was observed when the solution became cloudy. The turbidity of the solution was caused by the formation of insoluble polymer-rich domains. The time when the transparency of the solution completely disappeared was recorded as a clouding point. Except for MC14 and MC17, all preparations had a clouding point between 30 min and 6 h. We found that the clouding point was associated with the domain size of the resulting monoliths. When the solution

(21) Torres, F. E.; Troian, S. M. *Colloids Surf., A* **1994**, *89*, 227–239.
(22) Troian, S. M. *Phys. Rev. Lett.* **1993**, *71*, 1399–1402.
(23) Puri, S. J. *J. Phys.: Condens. Matter* **2005**, *17*, R101–R142.

Table 3. Characteristics of Mesopores

sample ID	surface area (m^2/g)	pore size (nm)	pore volume (cm^3/g)
MC3	331.6	8.0	0.41
MC4	349.5	8.0	0.45
MC6	347.2	8.1	0.44
MC7	361.2	8.3	0.43
MC8	323.4	7.8	0.41
MC9	345.8	8.1	0.44
MC10	331.3	7.8	0.43
MC11	337.1	7.9	0.45
MC12	351.6	8.0	0.44
MC13	348.9	8.1	0.43
MC15	344.7	8.1	0.43
MC16	338.4	8.0	0.45
MC18	420.3	8.5	0.56

clouded within a short period in the air bath, coarse domains with spherical morphologies developed. For example, MC6, MC11, and MC12 had clouding points of 30 min, 1 h, and 2 h; all three samples had spherical morphologies with grain sizes of 20, 5, and 2 μm. When the clouding point occurred after 3 h, the morphologies of the resulting monoliths were bicontinuous structures with fine domains. Finer structures were resulting from higher air-bath temperature or longer prepolymerization time. Phenomenologically, the formation of fine bicontinuous monolith was always accompanied by a long clouding point. MC10 and MC16 were prepared according to the recipe of MC4 with longer prepolymerization time and higher air-bath temperature. The corresponding clouding points of MC10 and MC16 were 6 and 5 h, respectively. Compared with the 3.5 h of MC4, the clouding points of MC10 and MC16 occurred much later. The domain sizes of MC10 and MC16 were much finer than those of MC4. The characteristics of domain sizes were detailed in Table 2. The textures of samples MC4, MC10, and MC16 were visualized in Figures 3D, 3F, and 6B.

Mesopore and Heating Treatment. Apart from various sizes and morphologies of macropores, all carbon rods had a uniform mesopore size distribution around 8 nm. The mesopores rendered high surface areas to these carbon rods (about 350 m^2/g). The pore volumes at 0.95 P/P_0 were about 0.45 cm^3/g. Sample MC18 had a slightly higher surface area and pore volume than other samples. This observation could be attributed to the elimination of the wall effect. The detailed characteristics of the mesopores were tabulated in Table 3. The carbon resulting from MC4 was further heated to 2600 °C. No obvious dimensional change was found except for the mesopores that were slightly shrunk from 8 to 6.5 nm. The high-temperature heating treatment resulted in graphitic structures as shown in the PXRD patterns in Figure 8. The carbon prepared at 850 °C had two broad diffraction peaks at 2θ of 24.5° and 43.2°. Such a PXRD pattern indicated that the carbon made at 850 °C was an amorphous carbon. The sample heat-treated to 2600 °C showed distinguished graphitic carbon characteristics with a sharp peak at 2θ of 26° and three differentiable peaks at high 2θ angles that revealed a highly crystalline structure.

Discussion

The formation of macropores through spinodal decomposition was studied in many polymeric and inorganic systems.[8,14,24,25] The bicontinuous appearance of microstructures in the resulting carbon certainly suggested a spinodal decomposition mechanism. The uniform mesopores were independent of the composition, temperature, and polymerization history. The size and uniformity of the mesopores strongly suggested that the mesopores were formed by a soft-template approach[1,20,26−28] in which the triblock copolymer formed a micelle structure with the phloroglucinol/formaldehyude resin through hydrogen bonding.[20,26] The underpinning physics of soft-template approach is the microphase separation. Thus, all of these results can be reconciled with a model in which two phase separations, i.e., microphase separation and spinodal decomposition, occurred concurrently in a single system. We denoted the coupling of microphase separation with spinodal decomposition as "dual phase separation". As illustrated in Scheme 1, in a dual phase separation system, the macropores and carbon skeletons were formed through spinodal decomposition and the mesopores were formed by microphase separation. A similar dual phase separation system with mixtures of organic and inorganic species was studied extensively by Nakanishi and Tanaka for the preparation of bimodal porous oxides.[5] The Nakanishi approach employed a sol−gel process for the preparation of mesopores, which was an inorganic polymerization system, while the system investigated in this paper was a distinct all-organic system.

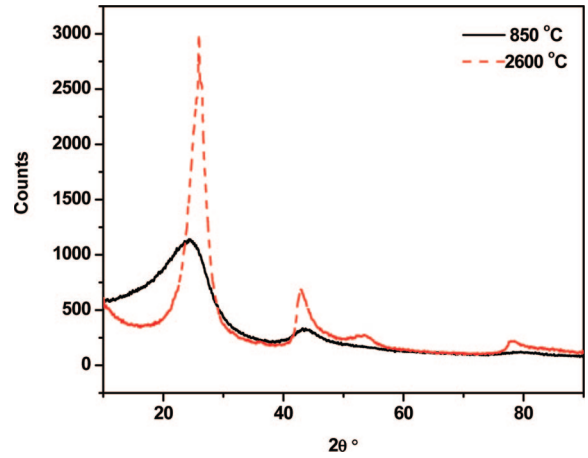

Figure 8. Powder X-ray diffraction patterns of a bimodal porous carbon heated at 850 °C (black solid line) and 2600 °C (red dashed line).

When phloroglucinol was mixed with triblock copolymer of PEO−PPO−PEO, phloroglucinol preferentially concentrated in the PEO domain of the block copolymer through hydrogen bonding. This mixture underwent microphase separation in selective solvents. As a result of the microphase separation, the PPO segments, which were the minor component in the mixture, aggregated and formed the cores of the micelles. The PEO domain incorporated with phlo-

(24) Hashimoto, T.; Takenaka, M.; Jinnai, H. *Polym. Commun.* **1989**, *30*, 177–179.
(25) Nakanishi, K. *J. Porous Mater.* **1997**, *4*, 67–112.
(26) Liang, C. D.; Hong, K. L.; Guiochon, G. A.; Mays, J. W.; Dai, S. *Angew. Chem., Int. Ed.* **2004**, *43*, 5785–5789.
(27) Meng, Y.; Gu, D.; Zhang, F. Q.; Shi, Y. F.; Yang, H. F.; Li, Z.; Yu, C. Z.; Tu, B.; Zhao, D. Y. *Angew. Chem., Int. Ed.* **2005**, *44*, 7053–7059.
(28) Zhang, F. Q.; Meng, Y.; Gu, D.; Yan, Y.; Yu, C. Z.; Tu, B.; Zhao, D. Y. *J. Am. Chem. Soc.* **2005**, *127*, 13508–13509.

Scheme 1. Schematic Illustration of Bimodal Porous Carbon Resulting from Dual Phase Separation

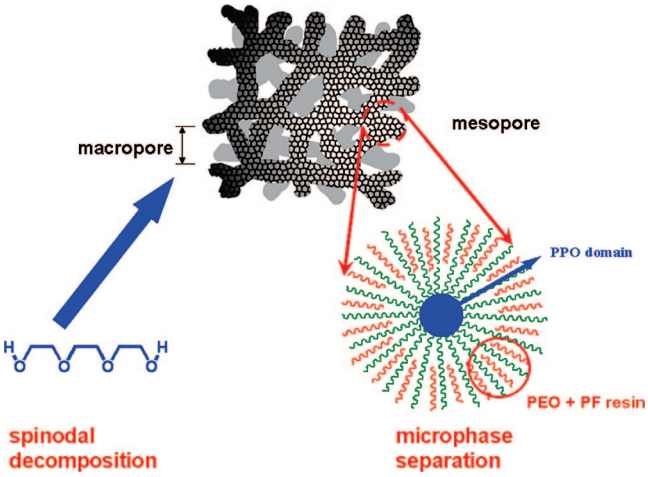

roglucinol and formed the matrix as the dominant component in the mixture. In the prepolymerization step, formaldehyde copolymerized with phloroglucinol and formed oligomers. The solubility of the polymer mixture in the alcoholic solution significantly decreased when phloroglucinol/formaldehyde (PF) oligomers formed. Thus, the polymer phase separated from the alcoholic solvents. Microphase separation occurred in the polymer phase that separated from the prepolymerization. This prepolymerization process is crucial for simplifying the synthesis system as we noticed that the block copolymer is sparely soluble in the glycolic solvent. Therefore, it is difficult to achieve a homogeneous solution with direct mixing of block copolymers and phloroglocinol in the glycolic solvent. The polymer mixtures from the prepolymerized PF oligomers and PEO−PPO−PEO are miscible with the glycolic solvents. Apparently, the PF oligomers promoted the solubility of PEO−PPO−PEO in glycolic solvents with an unknown mechanism. Formaldehyde was provided as an aqueous solution. The prepolymerization resulted in a homogeneous mixture of PEO−PPO−PEO and PF oligomers. This mixture was insoluble in water; therefore, water was excluded in the synthesis system. Water content in the solvents could greatly influence the spinodal decomposition.[14] The prepolymerization excluded the use of water and consequently simplified the solvents system. Miscibility of the polymer mixture with the glycolic solvents had a strong dependence on the molecular weights of the PF oligomers. Although we did not check the average molecular weights of the prepolymerized mixtures, we found that the duration of prepolymerization distinctly affected the spinodal decomposition.

After the single-phase mixture of P/F oligomers, PEO−PPO−PEO, and glycolic solvents was heated in the air bath, immiscibility progressively developed with concomitant polymerization. This process is known as polymerization-induced phase separation. Depending on the nature of the system, the phase separation could develop from spinodal decomposition or binodal decomposition.[8]The binodal decomposition resulted in isolated spherical domains. Most likely, the isolated spherical pores in samples MC1 and MC2 and discrete spherical particles in MC15 resulted from a binodal decomposition process. Bicontinuous microstructures

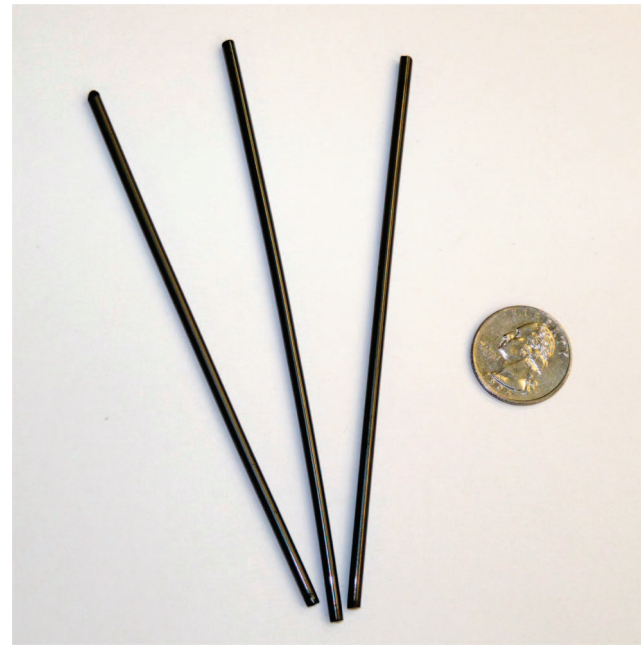

Figure 9. Photograph of three carbon monolithic rods; the HPLC column on the left side is for the purpose of showing the size of the rods.

of MC4, MC7, MC8, MC9, MC10, and MC16 ambiguously developed from the spinodal decomposition. Bicontinuous microstructures with spherelike or fused microspheres as seen in MC12 and MC13 could be the result of the boundary of spinodal and binodal phase separations. Miscibility is a major parameter governing the spinodal decomposition as we noticed that the immiscibility of the mixture occurred when the clouding point appeared. From the time when the clouding point appeared, the single-phase mixture developed into two phases: a solvent-rich phase and polymer-rich phase. These two phases gradually developed with the progress of polymerization. These results showed that the microstructures of the carbon were correlated with the clouding point. Preparations with long clouding points resulted in fine microstructures. The later the clouding points occurred, the longer the miscibility of the single-phase mixture was maintained. Evidently, the scale of domains depended on the miscibility of the mixture. The temperature of the air bath affected the spinodal decomposition through two factors: increased miscibility at higher temperature and increased polymerization rate of the PF oligomers. The increase of clouding points in MC15, MC4, and MC16 elucidated that the polymers and the glycolic solvents had high miscibility at elevated temperature. The scale of the microstructures decreased at high temperature. When the temperature was above 110 °C (sample MC17), immiscibility did not develop within 12 h. Therefore, no spinodal decomposition was observed in the investigated conditions. Secondary phase separation within the primary phase was observed in MC7. Secondary phase separation is a common phenomenon occurring in spinodal decomposition systems when the miscibility of the system is affected by other minor solvents.[14] With a short prepolymerization step, the polymer mixture separated from the ethanolic solution contained higher concentrations of water and ethanol than those polymers prepared after a long prepolymerization time. In the case of

MC7, the prepolymerized polymer was prepared within 30 min; therefore, water or ethanol dissolved in the prepolymerized polymer could be the minor solvents that caused the secondary phase separation.

The growth of domains in spinodal decomposition was significantly affected by an interface, which preferentially attracted one of the two domains. This effect was known in the literature as "wall effect".[21,22] We found that the wall effect could be avoided by aging the phase-separated mixture in a pure glycolic solvent without contacting the container. Therefore, in our system, the wall effect did not develop in the earlier stage of the spinodal decomposition.

All carbon materials with bicontinuous microstructures were rigid structures. Shown in Figure 9 is a photo of three carbon monolithic rods synthesized inside glass tubes with 7 cm i.d. and length of 20 cm. The U.S. quarter coin on the right side of the photo is employed to demonstrate the size of the carbon rods. The shiny surface of the carbon rods is as smooth as a mirror. We did not observe cracks during the handling, drying, and carbonization of the polymer rods. Heating treatment up to 2600 °C deteriorated neither the macropores nor the mesopores.

Conclusions

Bimodal porous carbon monoliths were synthesized through a dual phase separation process in which microphase separation occurred in the polymer phase and spinodal decomposition progressively developed through the cross-linking of the corresponding polymer mixture. As a result of this dual phase separation, macropores evolved from the solvent-rich phase and the mesopores were rendered after the pyrolysis of block copolymer templates. The sizes of the macropores and skeletons varied with reaction temperatures, prepolymerization times, and solvent compositions, whereas the mesopores tended to be independent of the spinodal decomposition process. This dual phase separation process offers a versatile method for the synthesis of bimodal porous carbon materials with tunability in two discrete length scales without interactive influences. Stable rigid structures were obtained even after treatment at extremely high temperature.

Acknowledgment. This research was sponsored by the Division of Chemical Sciences, Office of Basic Energy Sciences, U.S. Department of Energy under Contract DE-AC05-00OR22725 with Oak Ridge National Laboratory, managed and operated by UT-Battelle, LLC. The electron microscopic images were taken at the Center for Nanophase Materials Sciences, which is sponsored at Oak Ridge National Laboratory by the Scientific User Facilities Division, Office of Basic Energy Sciences, U.S. Department of Energy.

CM900344H